Experimental and Numerical Study on Shear Properties of Timber-to-timber Joint Using a Dowel Reinforced with a Self-tapping Screw

Jie Shen,[a] Xudong Zhu,[a] and Jianbing Chen [b,*]

Herein, a beech wood dowel reinforced with a self-tapping screw (composite dowel in brief) is proposed. Composite dowels were welded into the predrilled holes by high speed rotation. Force-displacement curves were obtained using a single-shear and dual connection. A double-peaked pattern was found in the bearing process, indicating that the wooden dowel and the self-tapping screw had a synergistic bearing effect in the bearing process. Regarding the failure mode, the self-tapping screw and the wooden dowel were bent, whilst the default wooden dowel fractured. Further, the numerical simulation was carried out using the finite element analysis software ABAQUS, and the result differed from the test value by only 4.30%, showing a high prediction accuracy. The study of the bearing capacity of the composite dowels provides a theoretical basis for the practical application of wooden dowels reinforced by self-tapping screws.

DOI: 10.15376/biores.18.3.6118-6131

Keywords: Composite dowels; Shear performance; Numerical simulation

*Contact information: a: Yangzhou Polytechnic Institute, Jiangsu 225100, China; b: Suzhou University of Science and Technology, Suzhou 215009, China; *Corresponding author: szctt2009@163.com*

INTRODUCTION

With the development of wood engineering composite materials, especially the structural integrated wood and the orthogonal laminated wood, self-tapping screws have been widely used in beam-column connecting joints (Chen *et al*. 2019). The traditional dowel joint, as a green and low-carbon connection, has also been applied in connections to some extent (Hao *et al*. 2020; Bui *et al*. 2020; Li *et al*. 2020). In addition, a wood welding technique proposed by Professor Pizzi in France is also used in the field of wood connection (Bocquet *et al*. 2007, 2017; Girardon *et al*. 2014; Satoshi *et al*. 2017).

In the field of material and joint reinforcement, self-tapping screws are widely used to control cracks of glulam and to strengthen mortise and tenon joints. Compared with glulam beams not reinforced with tapping screws, the bearing capacity of glulam beams reinforced with self-tapping screws can be increased by up to 50% (Johan *et al*. 2005). Another study has shown that the self-tapping screw reinforced glulam improves the modulus (Petrycki and Salem 2020). A prominent advantage of the self-tapping screw reinforcement is its ability to increase ductility, realizing a relatively safe failure mode. Self-tapping screws with local threads may not significantly improve strength, but they can improve ductility, especially for glulam with cracks. A high level of ductility signifies a failure mode with less brittle failure characteristics (Zhang *et al*. 2019a,b). Self-tapping screws can also be used to improve the compressive bearing capacity of glulam. The length,

number, and arrangement of self-tapping screws are verified to generate a profound impact on the failure mode and the bearing capacity (Tang *et al.* 2021).

Wood welding refers to the transfer of heat from wood material to wood cells through frictional heat generation under certain external forces. It results in the softening and fusion of lignin and hemicellulose, the formation of a cross-networking lattice structure in the interface, and finally glue-free bonding after cooling and curing. The structural strength and stiffness of solid wood welded with dowels are better than that of perforated joints. The properties of the welded joints were influenced by rotation speed, inserting speed, and the diameters of the wood dowel and predrilled holes. According to the studies of Leban *et al.* (2008) and Kanazawa *et al.* (2005), the best welded parameters were rotation speed 1500 and 1800 rpm, inserting speed 10 to 15 mm/min, and the ratio of wood dowel and predrilled hole 0.8 (Kanazawa *et al.* 2005; Leban *et al*. 2008). Its connecting performance is comparable to that of joints with dowels coated with the glued surface (Segovia and Pizzi 2009). The crisscrossed laminates are by round dowels connected to 4×4 m wooden plates *via* rotary welding. A relatively larger stiffness is thereby obtained using fewer wood laminates (Bocquet *et al*. 2007). The wood welded by inclined dowels can be used indoors because it has good dry strength, but it cannot be used outdoors, which can be attributed to a reduced wet strength (Omrani *et al*. 2007). In the case of mortise and tenon joints commonly used in furniture, it is found that the same strength can be achieved by welding multiple round dowels. Besides, a higher joint strength can be obtained by combining multiple round dowels with welding (Mougel *et al.* 2011).

Based on the advantages of self-tapping screws and wood welding, a composite dowel consisting of beech and tapping screw is proposed. The composite dowel was welded into the predrilled hole by high speed rotation. In the pre-experiment, it was found that during the welding of dowel, a large torsional force was generated due to the high rotational speed of the dowel into the pre-drill hole. It was easy to cause the fracture of the dowel, especially when the insertion depth reached 70 mm or more (Zhu *et al*. 2017, 2018). Liu *et al.* (2019) found that the compressed wood could be used for the wooden dowel to reduce the probability of the dowel breaking in the welding process, and to improve the tensile strength of the welded joints. It was shown that the usage of beech having no imperfections, high strength, and high stability reduced the probability of breaking during the welding. Meanwhile, the special structure of the beech dowel embedded self-tapping screws can be used to form a composite dowel.

EXPERIMENTAL

Materials

The laminates were made of spruce-pine-fir (SPF) imported from North America. The wood was grade 2 material with a cross-section of 38×89 mm. The average density was 495 kg/m³ and the moisture content was 9.7%. The self-tapping screw had a galvanized surface and was 5.2 mm in diameter and 70 mm in length. The beech dowel was 12 mm in diameter, 100 mm in length, 2% in moisture content, and 703 kg/m³ in average density. The tapping screws were provided by Shanghai Meigu Handwei Hardware Company. The SPF and Zelkova dowels were provided by Suzhou Kunlun Lvjian Wood Structure Technology Company.

Experimental Design

Typical testing equipment employed in the work was as follows: cross-cut saw, microcomputer-controlled electronic universal mechanical testing machine with a maximum force of 100 kN, claw hammer, electric hand drill, bench drill, *etc*. The composite dowel was made of the beech dowel and the self-tapping screw, with the following processing steps.

(1) The beech dowel and self-tapping screws were used, where the beech dowel had a diameter of 12 mm and a length of 70 mm.

(2) The beech dowel was clamped vertically by means of a clamping device. A pre-drilled hole with a diameter of 3 mm and a depth of 70 mm was set in the center of the beech dowel with a table drill.

(3) By means of an electric hand drill, a self-tapping screw was screwed into the pre-drilled hole in the center of the beech dowel center to form the composite dowel.

(4) A pre-drilling hole with a diameter of 10 mm and a depth of 70 mm was set in the member.

(5) Then composite dowel was then screwed into the pre-drilling hole in the member by means of an electric hand drill for the purpose of connection.

An example of the composite dowel is shown in Fig. 1.

Fig. 1. Composite dowel

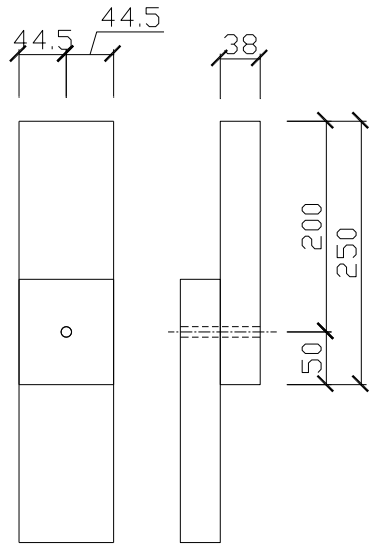

Fig. 2. Connection mode

In order to study the shear strength of the joint connected by the composite dowel, a single shear specimen was prepared with two lumber pieces connected with a single composite dowel, where the end distance is 50 mm and the side distance was 44.5 mm (Fig. 2). Regarding the composite dowel, a pre-drilling hole with a diameter of 10 mm was set in advance in the member to a depth of 70 mm. The table drill was then frictionally screwed into the member at a high speed of 1500 rpm with a feed rate of 10 mm/min (Bocquet *et al.* 2007, 2017), and three specimens are processed with this connection method (Fig. 3). The loading speed of the specimen was 5 mm/min.

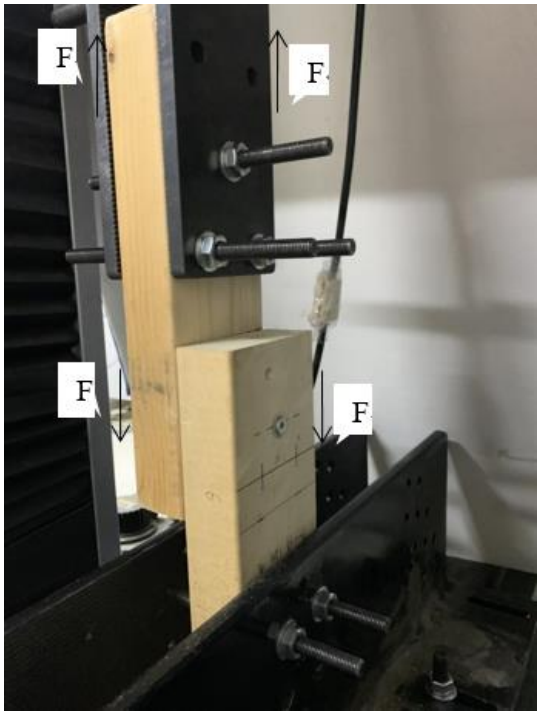

Fig. 3. Single shear specimen connected by composite dowel

RESULTS AND DISCUSSION

Shear Performance and Failure Mode

Combined with the initial stiffness analysis, it was found that the initial stiffness of the composite dowel was large, with its shear properties shown in Table 1.

Table 1. Shear Properties of Composite Dowel

Maximum Load (kN)	Yield Load (kN)	Ultimate Load (kN)	Initial Stiffness ($kN \cdot mm^{-1}$)	Final Deformation (mm)	Ductility Coefficient	Energy Dissipation (kN·mm)
4.230 (0.272)	2.051 (0.303)	3.641 (0.092)	0.877 (0.180)	20.940 (3.034)	5.009 (1.064)	68.309 (8.966)

Note: Standard deviation in brackets

A simple shearing test at the loading rate of 5 mm/min was used to obtain the force-displacement curve, as shown in Fig. 4. The maximum single shear load of the composite dowel joint member reached 4.23 kN, which was higher than the 2.977 kN of the joint connected by the default wood dowel. As shown in Fig. 4, there were two maximum peaks in the bearing capacity of the composite dowel joint members. The first maximum peak is the maximum load at the displacement 6-7 mm, while the second maximum peak reaches 3.7kN at the displacement 17-18mm. According to the previous study, the first maximum peak was similar to the force of wood dowel with diameter 12 mm, and the second maximum peak was similar to the force of self-tapping screw with diameter 5.2 mm.

When the single shear bearing capacity of the member reaches the first maximum value, there is no significant deformation of the joint. The slight sound of wood tearing is observed because of the shear tearing of the beech dowel under the small deformation of the joint during the load bearing process (Gao *et al*. 2019). However, due to the high

toughness of the embedded self-tapping screw, like the supporting role of steel bars in concrete (Yang *et al*. 2021), the beech dowel does not break completely or damage extensively. As the deformation continues to increase, the single shear bearing capacity of the member shows a declining stage. The bearing capacity of the beech dowel gradually decreases, while the tapping screws fail to fully exert their bearing capacity. With the further increase of deformation, the wall of the connection holes, the beech dowel, and the tapping screw reach a tight connection, and the bearing capacity tends to increase. Finally, when the second maximum value is reached, the self-tapping screw makes the maximum contribution to the bearing capacity of the joint. Meanwhile, as the dowel does not break completely, it still acts as a peripheral protection against large deformations of the self-tapping screws. However, after the second maximum value is reached, the load-bearing capacity of the joint decreases rapidly as the composite dowel breaks completely or is pulled out.

The final deformation indicates the displacement value when the load of the member drops to 80% of the maximum load. The final deformation of the composite dowel joint member is 20.987 mm. By Fig. 5, when the composite dowel joint member reaches the second maximum value, the self-tapping screw is subjected to a large load in advance due to the synergistic action of the combination of the tapping screws and the beech dowel. The joint dowel at this time is fractured or pulled out.

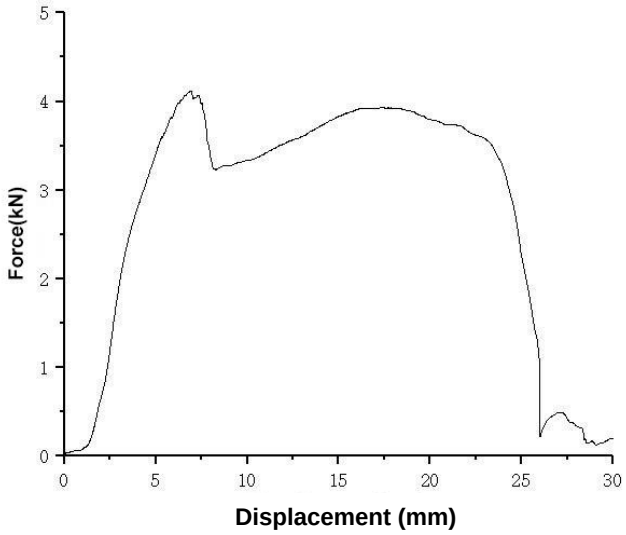

Fig. 4. Force displacement curve

Fig. 5. Failure pattern of composite dowel joint member

Finite Element Analysis

By means of modeling, the stress and deformation of the composite dowel under the action of single shear were analyzed. Simulation results were then compared with the experimental results to better analyze the stress characteristics of the joint mode.

(1) *Creation of model components*

In the modeling process, units should be unified at first. The unit system used in the simulation of length, force, density, stress, and time is mm, N, t/mm^3(10^{12}), N/mm^2, and s. Then, the three-dimensional model of each node component is created in the component module (Fig. 6), and the SPF specification material, self-tapping screw, and beech dowel are all set as deformable entities. Graphics are drawn on the two-dimensional interface in advance, and the length values are input to complete the three-dimensional model. The components with dowel holes are set. When creating self-tapping screws, the threads are ignored to increase the friction coefficient. The self-tapping screw is simplified to improve the convergence of the simulation (Hu *et al*. 2022a).

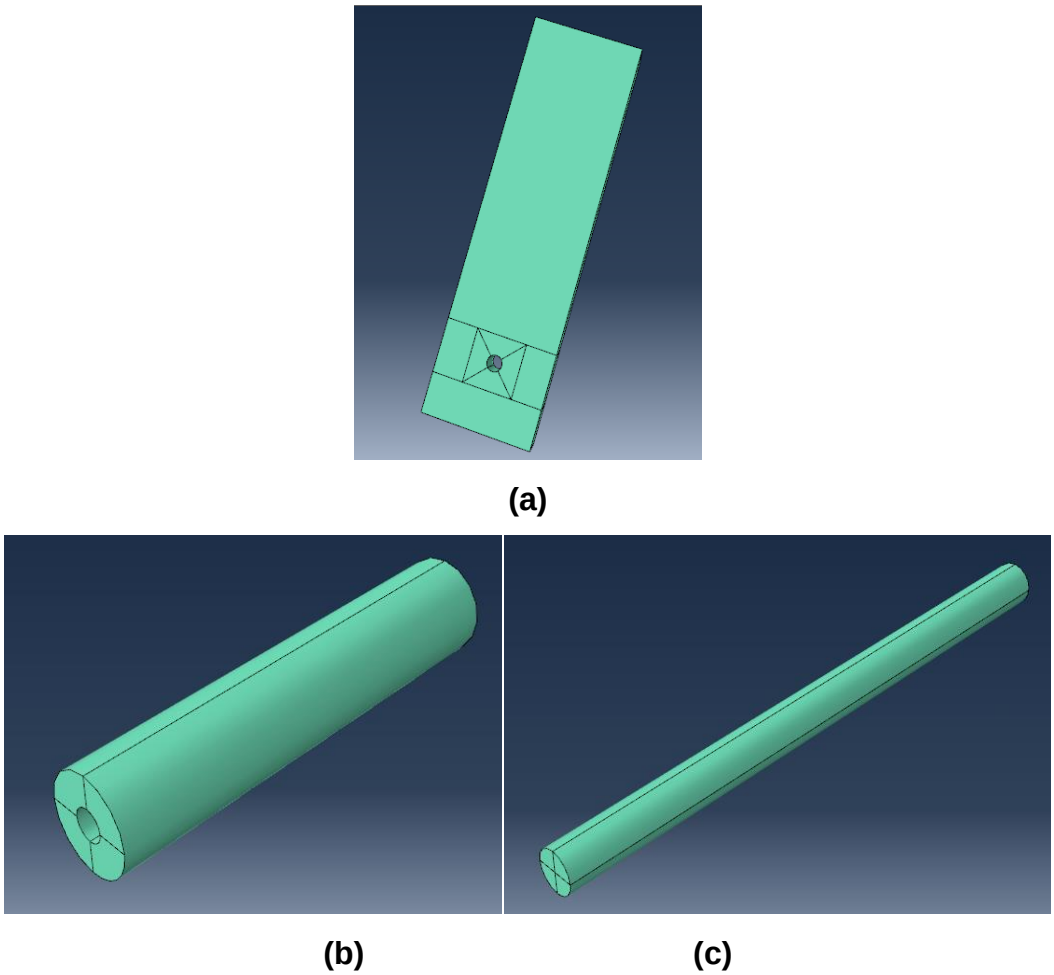

Fig. 6. Schematic diagram of component in finite element analysis (a) SPF (b) Beech (c)Tapping Screws

(2) *Defining material attributes*

1) SPF specification material

The relationship between the longitudinal and transverse components of the wood is shown in Figs. 7 and 8. The f_t and f_c parameters are the tensile and compressive ultimate strengths of wood, respectively. The ε_{tu}, ε_0, and ε_{cu} symbols indicate the tensile limit strain, compressive yield strain, and compressive limit strain of the wood along the grain, respectively. The $f_{c'}$ and $f_{cu'}$ parameters are the compressive yield strength and the compressive ultimate strength of wood stripes, respectively. The $\varepsilon_{0'}$ and $\varepsilon_{cu'}$ quantities are the compressive yield strain and ultimate strain of the wood along the transverse grain of wood, respectively.

Wood is an anisotropic material with complex mechanical properties, showing linear elasticity under low loads and plasticity under high loads. The varied stress directions in the wood lead to different forms of failure, *viz.* brittle failure by the tensile action and plastic failure in the compression. The elasticity and plasticity of wood thereby should be defined separately.

Regarding the material properties module, there are a number of elasticity types, including isotropy, anisotropy, engineering constants, *etc*. In this simulation, the orthogonal anisotropy of the wood is defined by the specified engineering constants. There are 9 model parameters to define the orthogonal anisotropy of the wood, including elasticity moduli E_1, E_2, and E_3 in three directions, three shear moduli G_{12}, G_{13}, and G_{23}, and three Poisson ratios of v_{12}, v_{13}, and v_{23}. As per the material property test, the longitudinal elastic modulus of the material with SPF specification is 5809 MPa, and the remaining elastic modulus and shear modulus can be converted by the proportional equation, as shown in Tab. 2, where subscripts 1, 2, and 3 respectively represent the longitudinal, radial, and chordal directions of the wood (Fig. 9). Poisson's ratios of the SPF component are recommended to be set as v_{12}=0.3, v_{13}=0.42, and v_{23}=0.30 (David *et al*. 2008).

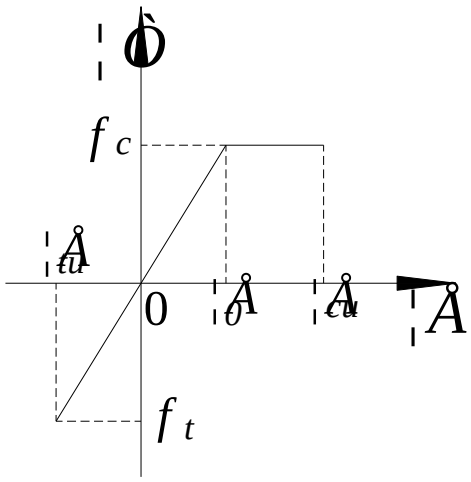

Fig. 7. Wood textural relation along grain

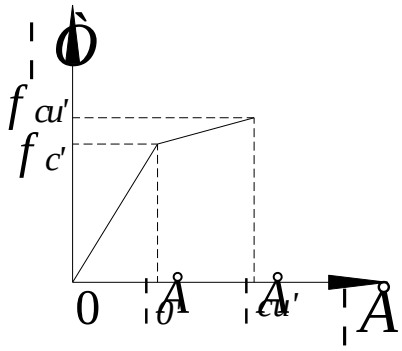

Fig. 8. Transverse grain constitutive relation of wood

Table 2. Model Parameters of SPF Specification Material

E_1 (GPa)	E_2 (GPa)	E_3 (GPa)	V_{12}	V_{13}	V_{23}	G_{12} (GPa)	G_{13} (GPa)	G_{23} (GPa)
5809	581	290	0.3	0.42	0.3	349	436	105

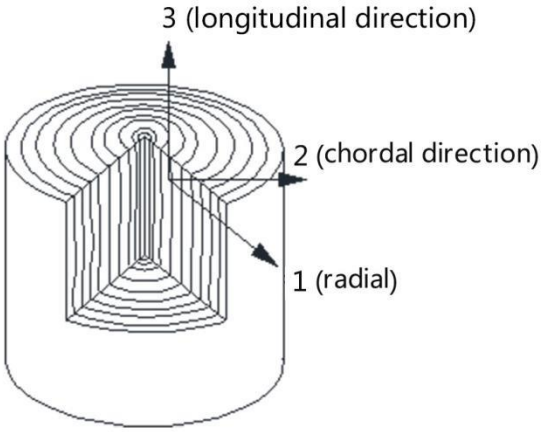

Fig. 9. Schematic diagram of wood

Plasticity is the property of a material to deform permanently under the external load. Wood is a kind of anisotropic and viscoelastic material. Under the action of tension, it shows a brittle failure with no plastic deformation. When wood is subjected to the compression, linear elastic characteristics appear in the initial stage of loading. With the increase of load, nonlinear characteristics begin to appear, showing a certain degree of plasticity. In ABAQUS, the plasticity of wood can be defined by a self-defined yield stress value ($\sigma°$) and six anisotropic yield pressure ratios (R_{11}, R_{22}, R_{33}, R_{12}, R_{13}, R_{23}). The yield pressure ratios are taken as Eq. 1 (Chen *et al*. 2011).

$$R_{11}=\frac{\sigma_{11}}{\sigma^0},\ R_{22}=\frac{\sigma_{22}}{\sigma^0},\ R_{33}=\frac{\sigma_{33}}{\sigma^0},\ R_{12}=\frac{\sigma_{12}}{\tau^0},\ R_{13}=\frac{\sigma_{13}}{\tau^0},\ R_{23}=\frac{\sigma_{23}}{\tau^0} \quad (1)$$

where σ_{ij} (i, j=1, 2, 3) indicates the measured yield stress, $\tau^0=\sigma^0/\sqrt{3}$.

$$L=\frac{1}{2}\left(\frac{1}{R_{22}^2}+\frac{1}{R_{33}^2}-\frac{1}{R_{11}^2}\right);\ M=\frac{1}{2}\left(\frac{1}{R_{11}^2}+\frac{1}{R_{33}^2}-\frac{1}{R_{22}^2}\right);\ N=\frac{1}{2}\left(\frac{1}{R_{11}^2}+\frac{1}{R_{22}^2}-\frac{1}{R_{33}^2}\right) \quad (2)$$

In Eq. 2, L, M, and N indicate the material constants.

According to the results of wood property tests, the plastic yield coefficient of the wood can be obtained by combining the above equations. Besides, the Hill yield criterion can only be met when the calculated results are positive.

2) Beech dowel

Based on the material property test and literature references (Hu *et al*. 2022b), the data in Table 3 were obtained as follows.

Table 3. Parameters of the Beech Dowel Model

E_1 (GPa)	E_2 (GPa)	E_3(GPa)	V_{12}	V_{13}	V_{23}	G_{12}(GPa)	G_{13} (GPa)	G_{23} (GPa)
12567	1374	579	0.450	0.554	0.841	899	595	195

3) Self-tapping screw

The self-tapping screw is simplified into an ideal elastic-plastic entity. Its stress-strain relationship is shown in Fig.10, where f_y is the yield strength of steel, taking 550 MPa. The value of ε_0 is 0.29%, and the Poisson's ratio is set as 0.3.

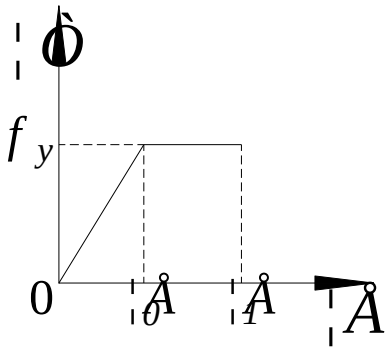

Fig. 10. Stress-strain relationship of tapping screw

(3) *Assemble components and define analysis steps*

In the module of assembling, components are respectively imported and connected into a whole by means of rotation, translation, array, and a series of other tools, as shown in Fig. 11.

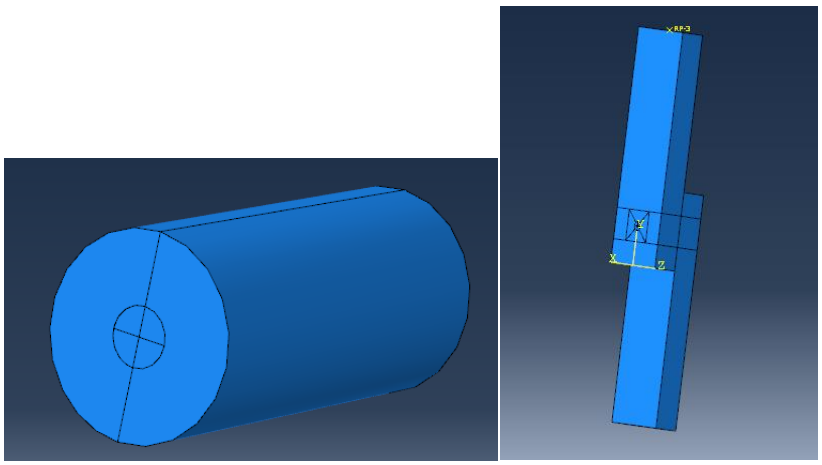

(a) **(b)**

Fig. 11. Assembly model drawing: (a) composite dowel, (b) Single shear specimen

When setting up the analysis step, the whole process is divided into two steps. In the first step, gravity is applied to the entire assembly and pressure is applied to the upper column end of the assembly. In the second step, a displacement is applied at the beam end, depending on the exact process of the monotonic loading test. In the analysis module, it is to select the type of "static, general analysis". When editing incremental steps, the maximum number of incremental steps is set as 10000, the initial incremental step is set as 0.01, the minimum incremental step is set as 10^{-5}, and the maximum incremental step is set as 0.5.

(4) *Interaction and load boundary setting*

The interaction modules have common contact and constraint functions. Contact occurs between surfaces, including the contact between SPF materials, the contact between SPF materials and tapping screws, the contact between SPF materials and the beech dowel, and the contact between the beech dowel and tapping screws. The contact in this model uses a "surface to surface contact", with contact attributes containing tangential action and normal action. The tangential action mainly considers the coefficient of friction, whilst the normal action defines the contact as a "hard contact". A reference point is drawn on the loading point of the SPF gauge material. The reference point is coupled to the surface of the gauge material.

The loading mode for this test is monotone displacement loading. In the boundary conditions, a fixed end constraint is established when testing the SPF specifications. The displacement load at the coupling point in the test direction is set during the analysis.

(5) *Division of cell grid*

To accurately and effectively simulate the force and deformation under loading, the entities of SPF specification wood, beech dowel, and self-tapping screws are meshed into grids, mainly using the hexahedral element C3D8I. There are three meshes in ABAQUS, which are respectively the structure optimization mesh, the sweep mesh, and the free mesh. When dividing complex structures, they are divided into regular geometries at first. Entities that cannot be divided by the grid partitioning are then swept. The grid division of each component is shown in Fig. 12.

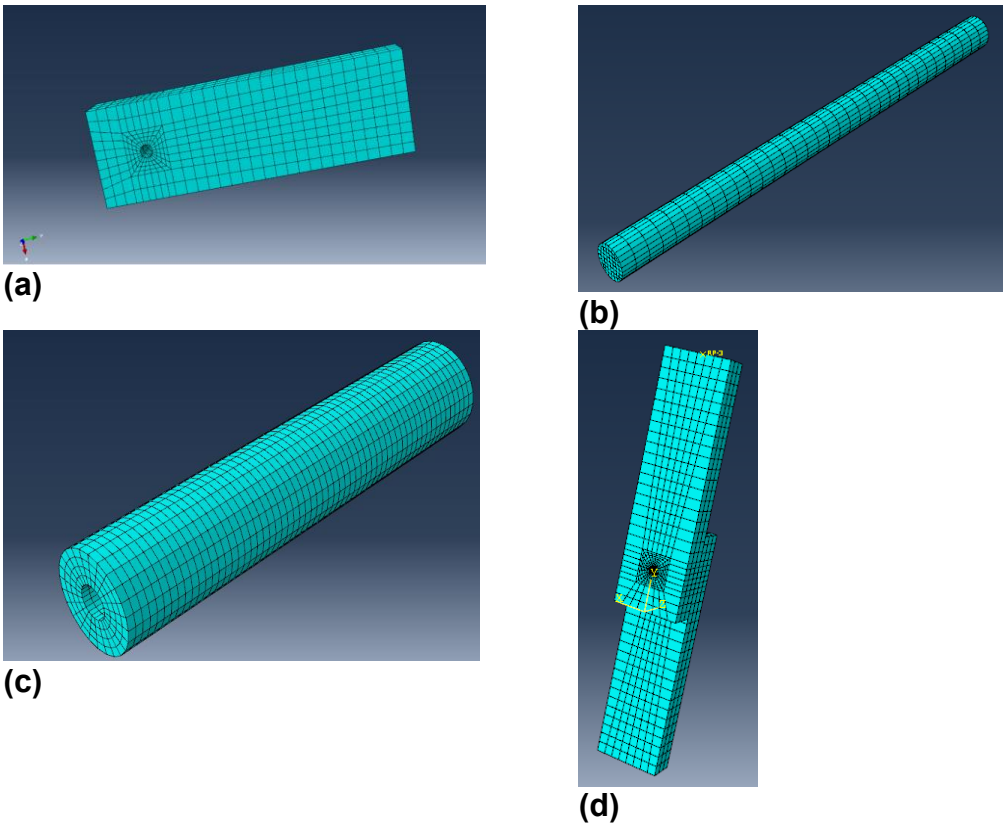

Fig. 12. Grid division diagram; SPF (a), Tapping screw (b), Beech dowel (c), and single shear Specimen (d)

(6) *Analysis and comparison of results*

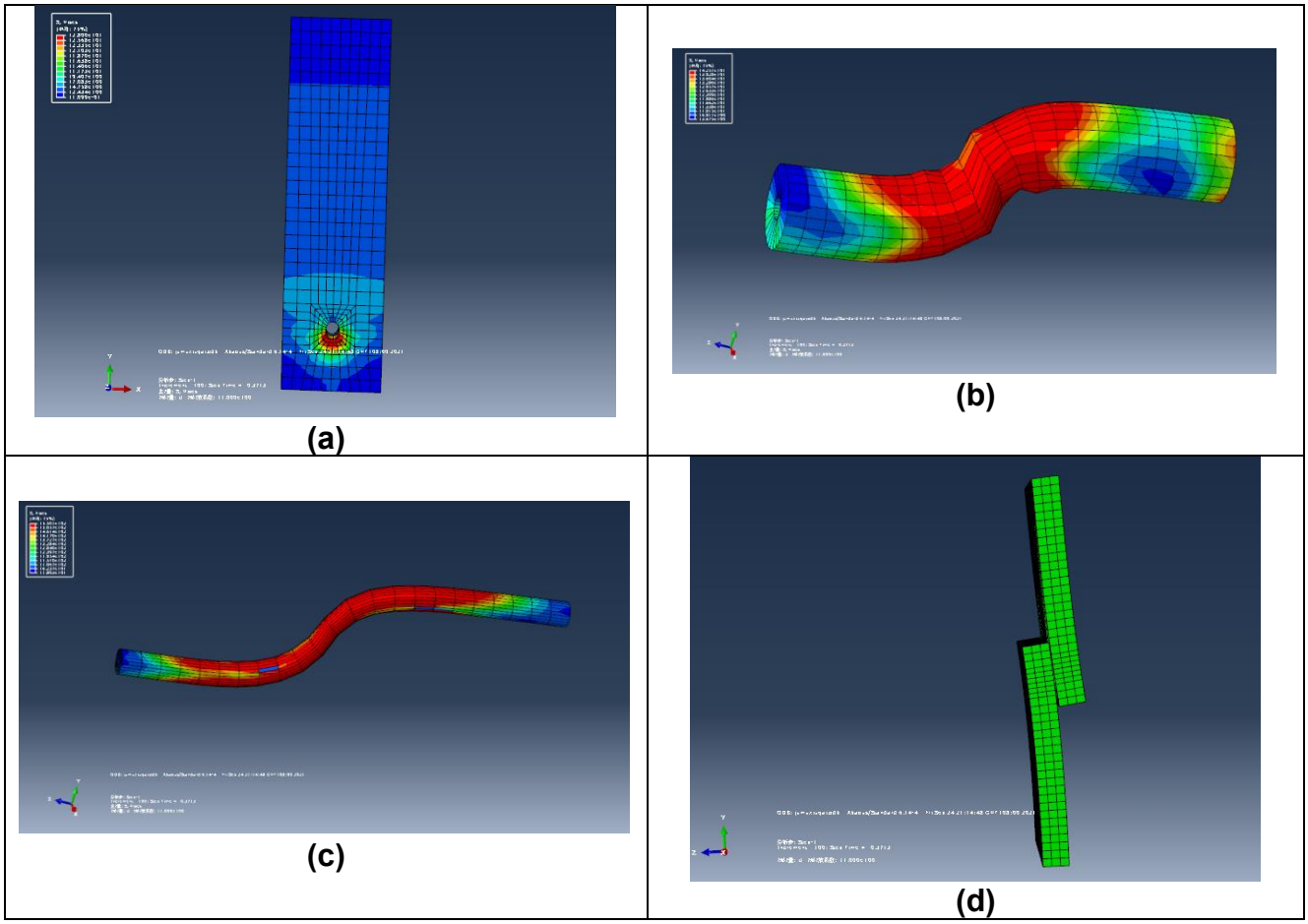

Fig. 13. Deformation cloud image; SPF (a), Beech (b), Tapping Screw (c) and single shear specimen (d)

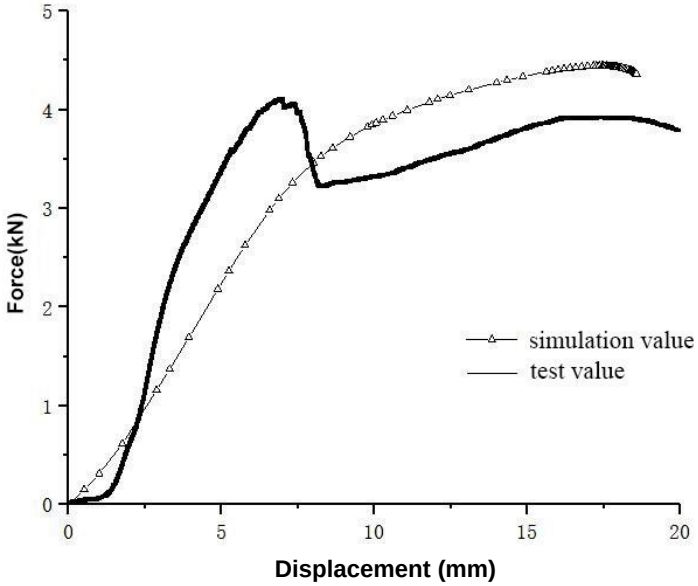

Fig. 14. Comparison of experimental and simulated shear capacity

The findings show that the joint members of the composite dowel have a good energy dissipation capacity. The composite dowels thereby can be applied to the common joint field of wood structure buildings. The deformation cloud map of each component, and the comparison and analysis of the simulated and experimental bearing capacity-displacement curve of the single shear component are presented. It simulates the reaming effect around the hole of the SPF material in the test process. During the first half of the loading, a good consistency is observed between the simulated value and the test value. However, unlike the joint failure mode in the test, the constitutive model of wood cannot directly simulate the formation and development of cracks. The simulation thereby shows no damage to the wood frame, and no first maximum peak value caused by the local failure of the beech dowel in the early stage. It makes the plastic properties obtained by the finite element simulation better than the experimental results. The maximum bearing capacity of the single shear specimen obtained by simulation is 4.447 kN, which differs from the test value of 4.23 kN by 4.30%, showing a good prediction accuracy.

CONCLUSIONS

1. Herein, a composite dowel prepared from beech wood and self-tapping screws is proposed. The study results showed that the joint members of the composite dowel had a good energy dissipation capacity.
2. Force-displacement curves were obtained using a single-shear approach. A double-peaked pattern was found in the bearing process, indicating that the wooden dowel and the self-tapping screw had a synergistic bearing effect. The ductility of the joint connected by composite dowel was attributable to the contribution of self tapping screw.
3. The numerical simulation was carried out using the finite element analysis software ABAQUS, and the result differed from the test value by only 4.30%, showing a high prediction accuracy. Due to the inability of the constitutive model of wood to directly simulate the formation and development of cracks, there was no failure phenomenon in the wood components. Therefore, the first maximum peak caused by local failure of the beech dowels in the early stage did not occur, which also resulted in better plastic properties obtained from finite element simulation than test results.
4. The study of the bearing capacity of composite dowels provides a theoretical basis for the practical application of composite dowels.

ACKNOWLEDGMENTS

The authors are grateful for the support of the National Natural Science Foundation of China (Grant No. 31901252), the Jiangsu Planned Projects for Postdoctoral Research Funds (Grant No. 2020Z075), the Science and Technology Program of Jiangsu Housing and Construction Department (Grant No. 2021ZD22), the Yangzhou Science and Technology Project (Grant No. YZ2022110), and the Natural Science Foundation of the High Education Institutions of Jiangsu Province (Grant No. 22KJA220003). The authors thank TopEdit (www.topeditsci.com) for linguistic assistance during the preparation of this manuscript.

REFERENCES CITED

Bocquet, J. F., Pizzi, A., Despres, A., Mansouri, H. R., Resch, L., Michel, D., and Letort, F. (2017). "Wood joints and laminated wood beams assembled by mechanically-welded wood dowels," *Journal of Adhesion Science and Technology* 21(3/4), 301-317. DOI: 10.1163/156856107780684585

Bocquet, J. F., Pizzi, A., and Resch, L. (2007). "Full-scale industrial wood floor assembly and structures by welded-through dowels," *European Journal of Wood and Wood Products* 65(2), 149-155. DOI: 10.1007/s00107-006-0170-4

Bui, T. A., Oudjene, M., Lardeur, P. Khelifa, M., and Rogaume, Y. (2020). "Towards experimental and numerical assessment of the vibrational serviceability," *Engineering Structures* 216, 1-10. DOI: 10.1016/j.engstruct.2020.110586

Chen, H., Liu, Z. B., Su, S. Z., and He, X. P. (2019). "Research review on connection performance of new tapping screws in wood structures," *Shanxi Architecture* 45(1), 34-35. DOI: 10.13719/j.cnki.cn14-1279/tu.2019.01.020

Chen, Z. Y., Zhu, E. C., and Pan, J. L. (2011). "Numerical simulation of mechanical behaviour of wood under complex stress," *Chinese Journal of Computational Mechanics* 28(04), 629-634+640. DOI: 10.7511/jslx201104024

David, W. G., Jerrold, E. W., and David, E. K. (2008). *Wood Handbook: Wood as an Engineering Material*, Forest Products Laboratory. DOI:10.2737/fpl-gtr-113

Gao, L. L., Xu, W., Li, R. R., and Huang, Q. T. (2019). "Study on influencing factors of joint strength of T-shaped elliptic tenon members," *Forest Products Industry* 56(10), 19-22. DOI: 10.19531/j.issn1001-5299.201910004

Girardon, S., Barthram, C., Resch, L., Bocquet, J. F., and Triboulot, P. (2014). "Determination of shearing stiffness parameters to design multi-layer spruce beams using welding-through wood dowels," *European Journal of Wood and Wood Products* 72(6), 721-733. DOI: 10.1007/s00107-014-0834-4

Hao, J. X., Xu, L., Wu, X. F., and Li, X. J. (2020). "Analysis and modeling of the dowel connection in wood T type joint for optimal performance," *Composite Structures* 253, 1-11. DOI: 10.1016/j.compstruct.2020.112754

Hu, W. G., Liu, Y., and Konukcu, A. C. (2022a). "Study on withdrawal load resistance of screw in wood-based materials: Experimental and numerical," *Wood Material Science & Engineering*. DOI: 10.1080/17480272.2022.2084699

Hu, W. G., Yu, R. Z., Luo, M. Y., and Konukcu, A. C. (2022b). "Study on tensile strength of single dovetail joint: Experimental, numerical, and analytical analysis," *Wood Material Science & Engineering*. DOI: 10.1080/17480272.2022.2155872

Johan, J. (2005). "Load carrying capacity of curved glulam beams reinforced with self-tapping screws," *Holz. als Roh- und Werkstoff* 63, 342-346. DOI: 10.1007/s00107-005-0016-5

Kanazawa, F., Pizzi, A., Properzi, M., Delmotte, L., and Pichelin, F. (2005). "Parameters influencing wood-dowel welding by high-speed rotation," *J. Adhes. Sci. Techno*l. 19(12), 1025-1038. DOI: 10.1163/156856105774382444

Leban, J.-M., Mansouri, H. R., Omrani, P., and Pizzi, A. (2008). "Dependence of dowel welding on rotation rate," *Holz. Roh. Werkst*. 66(3), 241-242. DOI: 10.1007/s00107-008-0228-6

Li, Q., Song, H., and Wang, Z. Q. (2020). "Study on flexural performance of composite wooden beams with bamboo/wood pins," *Journal of Northwest Forestry University* 35(2), 218-222. DOI: 10.3969/j.issn.1001-7461.2020.02.33

Liu, Q. (2019). "Research on the drawing resistance of compression wood pin in rotary friction welding," *Dalian: Dalian University of Technology*2019.

Mougel, E., Segovia, C., Pizzi, A., and Thomas, A. (2011). "Shrink-fitting and dowel welding in mortise and tenon structural wood joints," *Journal of Adhesion Science and Technology* 25(1-3), 213-221. DOI: 10.1163/016942410X503320

Omrani, P., Bocquet, J. F., Pizzi, A., Leban, J. M., and Mansouri, H. (2007). "Zig-zag rotational dowel welding for exterior wood joints," *Journal of Adhesion Science and Technology* 21(10), 923-933. DOI: 10.1163/156856107781393910

Petrycki, A., and Salem, S. (2020). "Structural integrity of bolted glulam frame connections reinforced with self-tapping screws in a column removal scenario," *Journal of Structural Engineering* 146(10), 1-13. DOI: 10.1061/(ASCE)ST.1943-541X.0002792

Satoshi, F., Keita, O., Masaki, N., Mariko, Y., and Yasutoshi, S. (2017). "Shear properties of metal-free wooden load-bearing walls using plywood jointed with a combination of adhesive tape and wood dowels," *European Journal of Wood and Wood Products* 75(3), 429-437. DOI: 10.1007/s00107-016-1084-4

Segovia, C., and Pizzi, A. (2009). "Performance of dowel-welded wood furniture linear joints," *Journal of Adhesion Science and Technology* 23(9), 1293-1301. DOI: 10.1163/156856109X434017

Tang, L. Q., Xu, W., Yang, H. F., Tan, G. H., and Chen, Y. (2021). "Test on transverse stress performance of glulam reinforced by tapping screws," *Journal of Nanjing University of Technology (Natural Science Edition)* 43(1), 94-100. DOI: 10.3969/j.issn.1671-7627.2021.01.014

Yang, Z., Yang, Q., and Bao, L. (2021). "Experimental study on seismic damage of joints in assembled monolithic reinforced concrete frames," *Industrial Architecture* 51(01), 54-60. DOI: 10.13204/j.gyjzG20190926006

Zhang, C., Guo, H. B., Jung, K., Harris, R., and Chang, W. S. (2019a). "Screw reinforcement on dowel-type moment-resisting connections with cracks," *Construction and Building Materials* 215, 59-72. DOI: 10.1016/j.conbuildmat.2019.04.160

Zhang, C., Guo, H. B., Jung, K., Harris, R., and Chang, W. S. (2019b). "Using self-tapping screw to reinforce dowel-type connection in a timber portal frame," *Engineering Structures* 178, 656-664. DOI: 10.1016/j.engstruct.2018.10.066

Zhu, X. D., Gao, Y., Yi, S. L., Ni, C., Zhang, J. R., and Luo, X. Y. (2017). "Mechanics and pyrolysis analyses of rotation welding with pretreated wood dowels," *Journal of Wood Science* 63(3), 216-224. DOI: 10.1007/s10086-017-1617-4

Zhu, X. D., Xue, Y. Y., Zhang, S. J., Zhang J., Shen, J., Yi, S. L., and Gao, Y. (2018). "Mechanics and crystallinity/thermogravimetric investigation into the influence of the welding time and $CuCl_2$ on wood dowel welding," *BioResources* 13(1), 1329-1347. DOI: 10.15376/biores.13.1.1329-1347

Article submitted: April 7, 2023; Peer review completed: April 29, 2023; Revised version received: July 13, 2023; Accepted: July 14, 2023; Published: July 25, 2023.
DOI: 10.15376/biores.18.3.6118-6131